# A phenomenological thermodynamic energy density function for ferroelectric wurtzite $Al_{1-x}Sc_xN$ single crystals

Yijia Gu[1,*], Andrew C. Meng[2], Aiden Ross[3] and Long-Qing Chen[3]

1. Department of Materials Science and Engineering, Missouri University of Science and Technology, Rolla, MO, 65409

2. Department of Physics and Astronomy, University of Missouri, Columbia, MO, 65211

3. Department of Materials Science and Engineering and Materials Research Institute, The Pennsylvania State University, University Park, PA, 16802

[*] Corresponding author, email: yijia.gu@mst.edu

## ABSTRACT

A Landau-Devonshire thermodynamic energy density function for wurtzite aluminum scandium nitride ($Al_{1-x}Sc_xN$) solid solution is developed. It is parametrized using available experimental and theoretical data, enabling the accurate reproduction of composition-dependent ferroelectric properties, such as spontaneous polarization, dielectric permittivity, and piezoelectric constants, for both bulk and thin films. The maximum concentration of Sc for the wurtzite structure to remain ferroelectric is found to be 61 at%. A detailed analysis of $Al_{1-x}Sc_xN$ thin films reveals that the ferroelectric phase transition and properties are insensitive to substrate strain. This study lays the foundation for quantitative modeling of novel ferroelectric wurtzite solid solutions.

## 1. INTRODUCTION

Recent demonstrations of wurtzite ferroelectrics based on AlN[1] and ZnO[2] have focused on their large remanent polarization (~ 100 μC $cm^{-2}$), which provide an increased memory window for neuromorphic computing applications. Structurally, the wurtzite crystal structure (space group $P6_3mc$) exhibits an intrinsic spontaneous polarization along its c-axis, which is very difficult to reversibly switch through application of an electric field[3]. Substitutional alloying of non-ferroelectric rocksalt phases such as ScN in AlN[1] and MgO in ZnO[2] are thought to increase their structural disorder to facilitate polarization switching, and have been observed to significantly improve ferroelectric properties, including large remanent polarizations (~100 μC $cm^{-2}$) and an almost ideal square-like hysteresis[1].

The ferroelectric properties of wurtzite-rocksalt alloys such as AlScN are of great interest due to their potential integration with semiconductor technologies. Aluminum scandium nitride ($Al_{1-x}Sc_xN$), for example, offers a seamless fit with GaN technology and holds promise for potential CMOS back-end-of-line integration[4]. Furthermore, the material's scalability down to 5 nm [5] positions ferroelectric $Al_{1-x}Sc_xN$ as an ideal candidate for the next generation of three-dimensional computing architecture, which could operate at low voltages and achieve higher memory densities. Such advancements promise faster computing speed and substantial energy savings. While these properties have implications for wide-ranging device applications from non-volatile memory to MEMS technologies, there are many remaining questions about ferroelectric behavior in wurtzite materials.

The absence of a reliable thermodynamic description under electric fields and strain is a significant challenge towards understanding the dynamics of ferroelectric switching in wurtzite ferroelectrics. The phase stability of $Al_{1-x}Sc_xN$ shows a complex dependence on Sc concentration. First, there is a structural transition from wurtzite to rocksalt at 30~40 at% Sc[6,7]. Second, there exists a limited composition range within which the wurtzite solid solution phase remains ferroelectric. On the wurtzite-rich region, the material typically becomes very difficult to switch due to the dielectric breakdown under a high field, and on the rocksalt-rich region, there can be structural instabilities such as compositional segregation or phase separation[7]. Determining this composition range typically requires a combination of extensive experimental work and first-principles calculations[8,9].

In this work, we develop a thermodynamic energy density function for wurtzite ferroelectric $Al_{1-x}Sc_xN$ single crystals. Utilizing this thermodynamic energy density function, we aim to bridge the knowledge gap concerning the influence of composition and strain on ferroelectric properties, i.e., the couplings among chemical, mechanical, and ferroelectric orders. This research does not only fill a crucial theoretical gap but also sets a foundation for developing thermodynamic energy density functions for a broader class of wurtzite-type ferroelectrics.

## 2. THERMODYNAMIC ENERGY DENSITY FUNCTION

We consider the simple case of a single substitutional alloying component of Sc on the Al sublattice, and the amount of Sc is described by the composition $x$. We adopted a six-order polynomial expression for the Landau-Devonshire energy density function. Using the high temperature paraelectric state as the reference, the free energy density of the ferroelectric state as a function of composition $x$, ferroelectric polarization $P_i$, and strain $\varepsilon_{ij}$ is expressed by

$$f(\varepsilon, P) = \alpha_{ij}(x)P_iP_j + \gamma_{ijkl}P_iP_jP_kP_l + \omega_{ijklmn}P_iP_jP_kP_lP_mP_n + \frac{1}{2}c_{ijkl}(\varepsilon_{ij} - \varepsilon^0_{ij})(\varepsilon_{kl} - \varepsilon^0_{kl}) \quad (1)$$

where $\alpha_{ij}$, $\gamma_{ijkl}$, and $\omega_{ijklmn}$ are the Landau expansion coefficients measured under the stress-free boundary conditions, $c_{ijkl}$ represents elastic stiffness tensor, and $\varepsilon^0_{ij}$ denotes the eigenstrain or spontaneous strain which is related to the spontaneous polarization. Under the stress-free condition, $\sigma_{ij} = 0$, the spontaneous strain is determined by the relative lattice parameter differences between the ferroelectric state and the paraelectric state both under the stress-free conditions and related to the spontaneous polarization through the electrostrictive effect, i.e.,

$$\varepsilon^0_{ij} = Q_{ijkl}P_kP_l \quad (2)$$

where $Q_{ijkl}$ is the electrostrictive tensor.

We chose the layered hexagonal structure (space group $P6_3/mmc$) as the unpolarized high symmetry centrosymmetric reference structure[10] because it is the intermediate structure when polarization vanishes during the switching between two wurtzite polar states (Fig. 1). Accordingly, the eigenstrain $\varepsilon^0_{ij}$ can also be deduced from the stress-free lattice constants (*a* and *c*) of the layered hexagonal structure and wurtzite structure, as shown below:

$$\varepsilon^0 = \begin{pmatrix} \varepsilon_{11}^0 & 0 & 0 \\ 0 & \varepsilon_{22}^0 & 0 \\ 0 & 0 & \varepsilon_{33}^0 \end{pmatrix} = \begin{pmatrix} \frac{1}{2}\left(\frac{a_W^2}{a_H^2} - 1\right) & 0 & 0 \\ 0 & \frac{1}{2}\left(\frac{a_W^2}{a_H^2} - 1\right) & 0 \\ 0 & 0 & \frac{1}{2}\left(\frac{c_W^2}{c_H^2} - 1\right) \end{pmatrix} \quad (3)$$

with subscripts $W$ and $H$ indicating wurtzite and layered hexagonal structures, respectively. Given that there are no spontaneous polarization components along the a- and b-axes in wurtzite structures ($P_1 = P_2 = 0, P_3 \neq 0$), the stress-free free energy density is simplified to

$$f(x, P_3) = \frac{1}{2}\alpha(x)P_3^2 + \frac{1}{4}\gamma P_3^4 + \frac{1}{6}\omega P_3^6 \quad (4)$$

where all the coefficients are considered composition-independent except for $\alpha$, which is assumed to vary linearly with Sc concentration $x$, such that $\alpha = \alpha_0(x - x_c)$, where $x_c$ is the critical concentration. This linear dependency is analogous to the temperature-induced ferroelectric phase transition in the conventional Landau-Devonshire model of ferroelectrics, where the coefficient of second-order term is linearly dependent on temperature, i.e., $\alpha = \alpha_T(T - T_0)$. However, given the Curie temperature ($T_0$) of $Al_{1-x}Sc_xN$ exceeds 1000 °C[11], small temperature variations at ambient conditions have a minimal impact on the its properties. Therefore, the temperature effect is not considered in this work since we focus on room temperature applications.

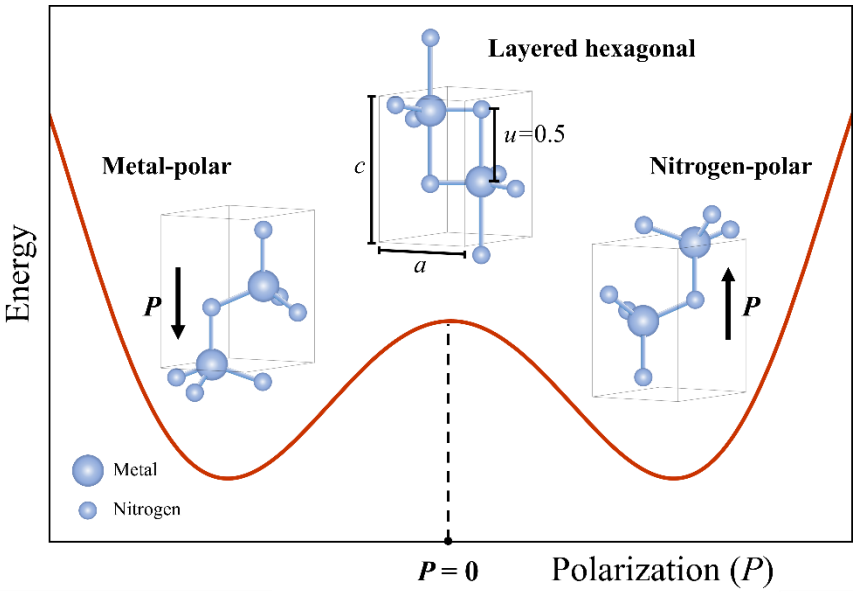


Figure 1. Free energy as a function of polarization of $Al_{1-x}Sc_xN$. The structures associated with respective polarization states are displayed schematically. *a* and *c* are lattice parameters, and *u* is the internal structure parameter. The layered hexagonal structure corresponds to the non-polar state.

The coefficients obtained are listed in Table 1. Values for $\alpha$, $\gamma$, and $\omega$ were determined using the properties of pure AlN, including dielectric constant[12], spontaneous polarization[10], and the free energy difference between wurtzite and layered hexagonal structures[12]. The critical concentration above which the material ceases to be ferroelectric, $x_c$, was derived using the polarization values calculated from first-principles calculations[8,13–15]. The elastic stiffness constants and the electrostrictive constants, applicable to $x \leq 0.5$, were from literature[16] and fitting[17], respectively.

Table 1. Coefficients of the Landau-Devonshire Potential

| Coefficient | Value | Unit |
|---|---|---|
| $\alpha_0$ | 5.50378 | GJ m $C^{-2}$ |
| $\gamma$ | 0.149031 | GJ $m^5$ $C^{-4}$ |
| $\omega$ | 0.928609 | GJ $m^9$ $C^{-6}$ |
| $x_c$ | 0.6115 | 1 |
| $c_{11}$ | $285.12x + 396(1-x) - 238.39x(1-x)$ | GPa |
| $c_{12}$ | $180.75x + 137(1-x) + 11.23x(1-x)$ | GPa |
| $c_{13}$ | $141.7x + 108(1-x) + 51.59x(1-x)$ | GPa |
| $c_{33}$ | $-155.17x + 373(1-x) + 95.49x(1-x)$ | GPa |
| $c_{44}$ | $176.44x + 116(1-x) - 158.8x(1-x)$ | GPa |
| $c_{66}$ | $52.19x + 129.5(1-x) - 124.81x(1-x)$ | GPa |
| $Q_{13}$ | $-0.00869634 - 0.0330153x + 0.12487x^2 - 0.335742x^3$ | $m^4$ $C^{-2}$ |
| $Q_{33}$ | $0.0203677 + 0.101335x - 0.389369x^2 + 1.07336x^3$ | $m^4$ $C^{-2}$ |

Note: $c_{66} = (c_{11} - c_{12})/2$

## 3. PROPERTIES OF STRESS-FREE SINGLE CRYSTALS

By minimizing the stress-free density function with respect to the ferroelectric polarization under zero electric field and zero stress, we obtain the magnitudes of ferroelectric spontaneous polarization $P_{sp}$,

$$P_{sp} = P_3 = \left(\frac{-\gamma \pm \sqrt{\gamma^2 - 4\alpha\omega}}{2\omega}\right)^{\frac{1}{2}} \tag{5}$$

Fig. 2(a) shows the variation of spontaneous polarization as a function of Sc concentration in the $Al_xSc_{1-x}N$ solid solution. As $\alpha, \gamma$, and $\omega$ are all positive, the ferroelectric transition occurring at $x_c$ is second order, as indicated by the continuous decrease of $P_{sp}$ to zero at $x_c$.

The relative permittivity (dielectric constant, $\epsilon_r$), obtained by the second derivative of the free energy density function with respect to $P_3$, is expressed as

$$\epsilon_r = 1 + \chi_{33} = \begin{cases} 1 + (\alpha\kappa_0)^{-1} & x > x_c, \text{Non} - \text{ferroelectric state} \\ 1 - \left(4\alpha + 2\gamma P_{sp}^2\right)^{-1}\kappa_0^{-1} & x < x_c, \text{ Ferroelectric state} \end{cases} \tag{6}$$

where $\kappa_0$ is the vacuum permittivity, and $\chi_{33}$ is the reciprocal dielectric susceptibility component along *c*-axis. Fig. 2(b) plots the relative permittivity as a function of Sc concentration, revealing a divergence at $x_c$. To the left of plot ($x < x_c$), the ferroelectric phase is stable. The curve to the

right of $x_c$ represents the relative permittivity of the non-ferroelectric phase. The divergence of the relative permittivity here is similar to the behavior of conventional ferroelectric materials at their Curie temperatures, which can be explained by the flattening of the overall energy landscape[18]. Experimental confirmation is needed to validate this predicted dielectric anomaly. Combining relative permittivity, spontaneous polarization and electrostrictive coefficient, the piezoelectric constant can be calculated using the following expressions,

$$d_{31} = d_{32} = 2\kappa_0\chi_{33}Q_{31}P_3 \quad (7a)$$

$$d_{33} = 2\kappa_0\chi_{33}Q_{33}P_3 \quad (7b)$$

Fig. 2(c) depicts the dependency of piezoelectric constant $d_{31}$ and $d_{33}$ on Sc concentration. The magnitudes of both piezoelectric constant components increase with Sc concentration. Since the piezoelectric constants are proportional to the corresponding relative permittivity, the piezoelectric constants also increase dramatically as the Sc concentration approaches the critical concentration $x_c$. Hence, piezoelectric coefficients are expected to reach maxima around $x_c$ as well. The piezoelectric constants calculated by Caro *et al* [19] are plotted for comparison, which show a similar trend as a function of Sc concentration.

Using Eq. (2), the spontaneous strain for $Al_{1-x}Sc_xN$ can be calculated by,

$$\varepsilon_{11}^0 = \varepsilon_{22}^0 = Q_{13}P_3^2, \varepsilon_{33}^0 = Q_{33}P_3^2 \quad (8)$$

Fig. 3(a) shows the spontaneous strain components $\varepsilon_{11}^0$ and $\varepsilon_{33}^0$ as functions of Sc concentration. Both components increase with Sc concentration. By combing Eq. (3) and (8), the lattice parameters for the reference layered hexagonal structure are calculated using the following derived relationship,

$$a_H = \left[2Q_{13}\left(\frac{-\gamma\pm\sqrt{\gamma^2-4\alpha\omega}}{2\omega}\right)+1\right]^{-1/2} a_W \quad (9a)$$

$$c_H = \left[2Q_{33}\left(\frac{-\gamma\pm\sqrt{\gamma^2-4\alpha\omega}}{2\omega}\right)+1\right]^{-1/2} c_W \quad (9b)$$

These lattice parameters are compared to those of wurtzite structures in Fig. 3(b). Since the lattice parameters of reference layered hexagonal structure are crucial for evaluating external strain, such as the epitaxial strain from the substrate for the thin film form, we fitted their dependence on Sc concentration using a third-order polynomial. Table 2 enumerates the lattice parameters for both the wurtzite[16] and the layered hexagonal structures as functions of Sc concentration $x$, for the range of $0 < x < 0.5$.

Table 2. Lattice Parameters of the Wurtzite Structure and the Layered Hexagonal Structure as Functions of Sc Concentration $x$ ($0 < x < 0.5$).

| | Lattice parameter (Å) |
|---|---|
| $a_W$[16] | $3.741x + 3.11(1-x) - 0.242x(1-x)$ |

| | |
|---|---|
| $c_W$[16] | $4.245x + 4.994(1-x) + 1.114x(1-x)$ |
| $a_H$ | $3.16412 + 0.415497x + 0.349071x^2 + 0.0514072x^3$ |
| $c_H$ | $4.80236 + 0.259264x - 1.74924x^2 + 0.267878x^3$ |

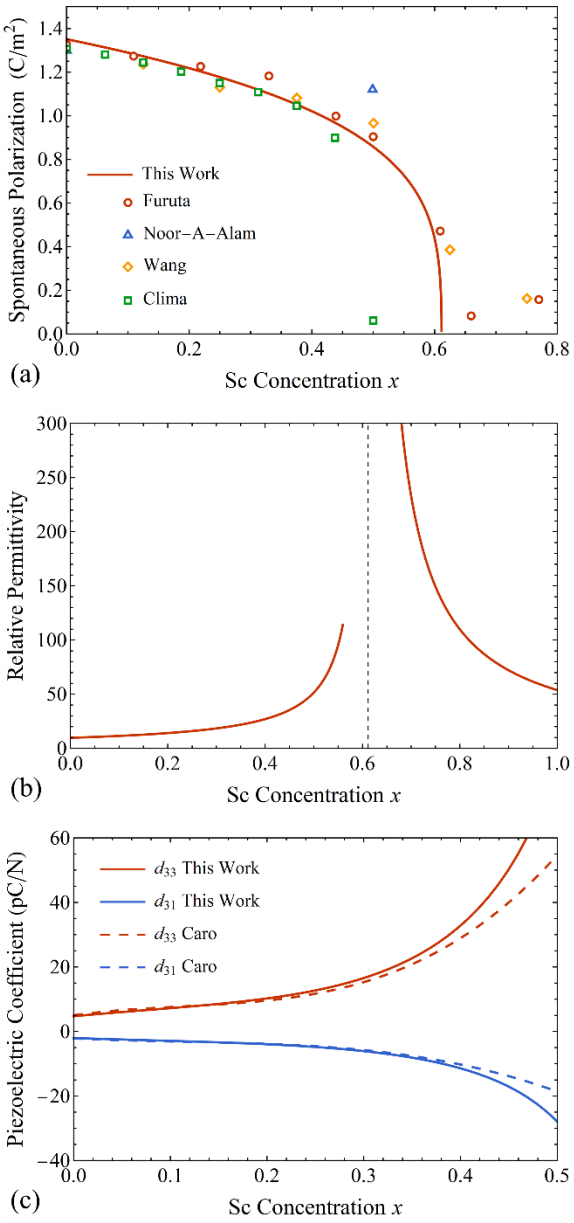


Figure 2. Ferroelectric properties of stress-free wurtzite $Al_{1-x}Sc_xN$ single crystals as functions of Sc concentration. (a) Spontaneous polarization. Symbols are taken from Furuta[8], Noor-A-Alam[13], Wang[15], and Clima[14]. (b) Relative permittivity. The dashed line indicates the critical concentration $x_c$. (c) Piezoelectric coefficients. The dashed lines are from Caro *et al* [19].

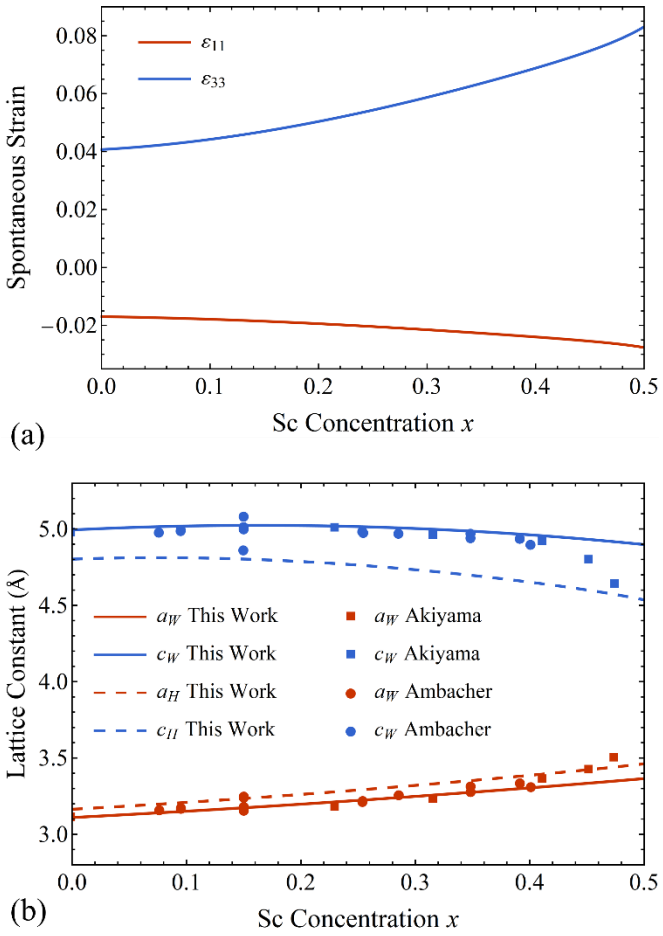


Figure 3. (a) Spontaneous strain of wurtzite $Al_{1-x}Sc_xN$ single crystals as a function of Sc concentration. (b) Lattice constant of wurtzite and reference layered hexagonal $Al_{1-x}Sc_xN$ single crystals as a function of Sc concentration. Symbols are taken from Akiyama *et al*'s[20] and Ambacher *et al*'s[16] experiments.

## 4. EFFECTS OF STRAIN ON THE PROPERTIES OF $AL_{1-x}SC_xN$ THIN FILM

As the applications of $Al_{1-x}Sc_xN$ are centered around the scaling of ferroelectric memory devices and electromechanical sensors and actuators for MEMS devices, existing $Al_{1-x}Sc_xN$ growth has largely been focused on thin films. In this section, we apply the developed thermodynamic energy density function to explore the properties of $Al_{1-x}Sc_xN$ in thin film form.

Under the biaxial thin film boundary condition[21], we have

$$\varepsilon_{11} = \varepsilon_{22} = \varepsilon_S, \varepsilon_{12} = \varepsilon_{21} = 0, \sigma_{13} = \sigma_{23} = \sigma_{31} = \sigma_{32} = \sigma_{33} = 0 \tag{10}$$

Solving Eq. (10) gives us

$$\sigma_{11} = \sigma_{22} = \left(c_{11} + c_{12} - \frac{2c_{13}^2}{c_{33}}\right)(\varepsilon_S - \varepsilon_1^0) \tag{11}$$

Thus, the expression for total energy density becomes

$$f = \frac{1}{2}\alpha' P_3^2 + \frac{1}{4}\gamma' P_3^4 + \frac{1}{6}\omega P_3^6 + \left(c_{11} + c_{12} - \frac{2c_{13}^2}{c_{33}}\right)\varepsilon_S^2 \tag{12}$$

where $\alpha' = \alpha - 4\left(c_{11} + c_{12} - \frac{2c_{13}^2}{c_{33}}\right)\varepsilon_S Q_{1133}$, and $\gamma' = \gamma + 4\left(c_{11} + c_{12} - \frac{2c_{13}^2}{c_{33}}\right)Q_{1133}^2$. Hence, the critical Sc concentration as a function of substrate strain $\varepsilon_S$ is given by

$$x_c' = x_c + 4\left(c_{11} + c_{12} - \frac{2c_{13}^2}{c_{33}}\right)\frac{Q_{1133}}{\alpha_0}\varepsilon_S \quad (13)$$

The ferroelectric phase diagram of wurtzite $Al_{1-x}Sc_xN$ is constructed with Sc concentration and biaxial substrate strain $\varepsilon_S$ as variables. As shown in Fig. 4, the phase boundary between ferroelectric and non-ferroelectric wurtzite shifts slightly at around x ~ 0.6 Sc concentration and is moderately affected by the substrate strains up to 10% compressive strain. It should be noted that the calculated ferroelectric phase diagram is based on the extrapolation of elastic stiffness constants and electrostrictive coefficient, which are valid up to an Sc concentration of $x < 0.5$. In addition, a rocksalt phase may also appear at 30~40 at% Sc regions[6,7], which is not considered in the current thermodynamic potential but could potentially be addressed using the CALPHAD model[22]. Future experimental work is needed to verify this phase diagram for $Al_{1-x}Sc_xN$ wurtzite ferroelectric thin films.

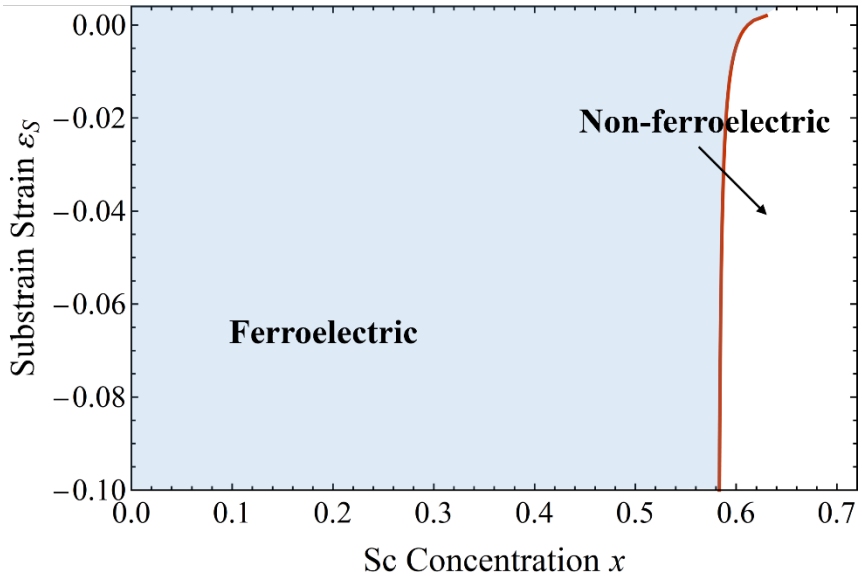


Figure 4. The substrate strain-composition phase diagram for $Al_{1-x}Sc_xN$ wurtzite ferroelectric thin films.

With the renormalized Landau expansion coefficients $\alpha'$ and $\gamma'$ under the thin film boundary condition, the combined effects of biaxial substrate strain and Sc concentration on the spontaneous polarization, relative permittivity, and piezoelectric constant are evaluated using Eq. (12). As the strain states of the grown thin films are mostly unavailable, we calculated the thin film properties for substrate strains ranging from -8.0% to 0%. As shown in Fig. 5, the calculated spontaneous polarization, relative permittivity, and piezoelectric constant are in good agreement with thin film experimental data[1,8,13–15,23–26], although they were not used for the fitting of the energy density function. The Sc concentration strongly affects the spontaneous

polarization, relative permittivity, and piezoelectric constant. The biaxial substrate strain does not show a strong influence on ferroelectric properties, especially the relative permittivity and the piezoelectric coefficients, in contrast to many perovskite ferroelectric thin films[27,28]. This limited influence is primarily attributed to the significantly larger magnitude of the second-order Landau coefficient $\alpha$, which is approximately two orders of magnitude greater than that of well-known perovskite ferroelectrics, such as $BaTiO_3$[29,30]. Therefore, the strain effect intensifies only as $x$ approaches $x_c$, where the magnitude of $\alpha$ dramatically decreases. Both relative permittivity and piezoelectric constants show sharp increases as $x$ approaches $x_c$, with their maxima occurring at lower substrate strains. Increased, compressive substrate strain tends to level out the variations in both relative permittivity and piezoelectric coefficients.

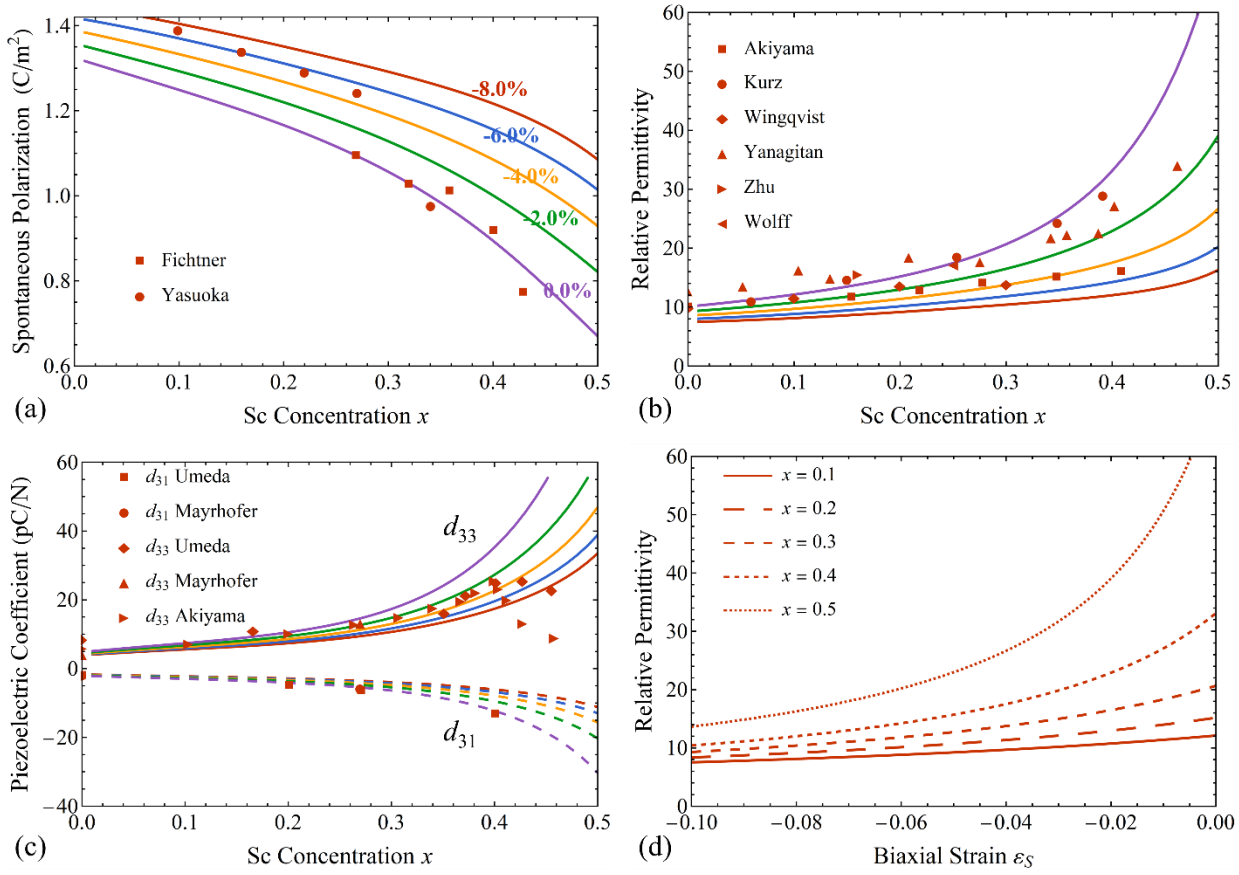


Figure 5. The properties of $Al_{1-x}Sc_xN$ wurtzite ferroelectric thin films. (a) Spontaneous polarization as a function of Sc concentration. Symbols are taken from Fichtner [1] and Yasuoka[23]. (b) Relative permittivity as a function of Sc concentration. Symbols are taken from Akiyama[31], Kurz[32], Wingqvist[33], Yanagitan[34], Zhu[3] and Wolff[35]. (c) Piezoelectric constants as a function of Sc concentration. Symbols are taken from Umeda[24], Mayrhofer[25], and Akiyama[26]. (d) Relative permittivity as a function of biaxial strain. All the solid and dashed lines are from our calculations. The line colors in (a-c) indicate different substrate strains, i.e., -8.0% (red), -6.0% (blue), -4.0% (orange), -2.0% (green), and 0 (purple), as indicated in (a).

## 5. CONCLUSIONS

In this work, we developed a Landau-Devonshire free energy density function for aluminum scandium nitride $Al_{1-x}Sc_xN$ using a layered hexagonal structure as the high-symmetry centrosymmetric reference state. By assuming that the second-order Landau coefficient is linearly dependent on the Sc concentration, the energy function accounts for the compositional effects on the total free energy. The parameters of the thermodynamic energy function are fitted to existing experimental and theoretical data. With composition-dependent elastic stiffness constants and electrostrictive coefficients, the free energy density function accurately reproduces the ferroelectric properties, including spontaneous polarization, relative permittivity, and piezoelectric coefficients. A divergence in the relative permittivity was observed at the critical composition where the ferroelectric transition occurs. We analyzed $Al_{1-x}Sc_xN$ thin films considering the effects of biaxial substrate strain and found that the strain has a minimal effect on the critical composition or the phase boundary between ferroelectric and non-ferroelectric wurtzite phases. This work demonstrates the feasibility of applying this composition-dependent Landau-Devonshire energy function to describe novel wurtzite-type ferroelectric solid solutions. This developed Landau-Devonshire energy function provides a starting point to quantitatively model $Al_{1-x}Sc_xN$ and can be further implemented in more complicated models such as the phase-field, allowing for the potential quantitative study of inhomogeneous ferroelectric switching and finite size effects which will stimulate the advancement and incorporation of these promising materials in microelectronic devices.

## ACKNOWLEDGEMENT

The authors would like to thank F. Xue for the helpful discussion. The effort by AR and LQC is partially supported by the National Science Foundation under DMR-2133373.

## DATA AVAILABILITY

The data that support the findings of this study are available from the corresponding author upon reasonable request.

## REFERENCES

[1] S. Fichtner, N. Wolff, F. Lofink, L. Kienle, and B. Wagner, "AlScN: A III-V semiconductor based ferroelectric," J. Appl. Phys. **125**(11), 114103 (2019).

[2] K. Ferri, S. Bachu, W. Zhu, M. Imperatore, J. Hayden, N. Alem, N. Giebink, S. Trolier-McKinstry, and J.-P. Maria, "Ferroelectrics everywhere: Ferroelectricity in magnesium substituted zinc oxide thin films," J. Appl. Phys. **130**(4), 044101 (2021).

[3] W. Zhu, J. Hayden, F. He, J.-I. Yang, P. Tipsawat, M.D. Hossain, J.-P. Maria, and S. Trolier-McKinstry, "Strongly temperature dependent ferroelectric switching in AlN, Al 1-x Sc x N, and Al 1-x B x N thin films," Appl. Phys. Lett. **119**(6), 062901 (2021).

[4] D. Wang, P. Wang, S. Mondal, S. Mohanty, T. Ma, E. Ahmadi, and Z. Mi, "An Epitaxial Ferroelectric ScAlN/GaN Heterostructure Memory," Adv. Electron. Mater. **8**(9), 1–8 (2022).

[5] J.X. Zheng, M.M.A. Fiagbenu, G. Esteves, P. Musavigharavi, A. Gunda, D. Jariwala, E.A. Stach, and R.H. Olsson, "Ferroelectric behavior of sputter deposited Al0.72Sc0.28N approaching 5 nm thickness," Appl. Phys. Lett. **122**(22), 0–7 (2023).

[6] S. Satoh, K. Ohtaka, T. Shimatsu, and S. Tanaka, "Crystal structure deformation and phase transition of AlScN thin films in whole Sc concentration range," J. Appl. Phys. **132**(2), 025103 (2022).

[7] X. Zhang, E.A. Stach, W.J. Meng, and A.C. Meng, "Nanoscale compositional segregation in epitaxial AlScN on Si (111)," Nanoscale Horizons, 674–684 (2023).

[8] K. Furuta, K. Hirata, S.A. Anggraini, M. Akiyama, M. Uehara, and H. Yamada, "First-principles calculations of spontaneous polarization in ScAlN," J. Appl. Phys. **130**(2), (2021).

[9] K.R. Talley, S.L. Millican, J. Mangum, S. Siol, C.B. Musgrave, B. Gorman, A.M. Holder, A. Zakutayev, and G.L. Brennecka, "Implications of heterostructural alloying for enhanced piezoelectric performance of (Al,Sc)N," Phys. Rev. Mater. **2**(6), 063802 (2018).

[10] C.E. Dreyer, A. Janotti, C.G. Van de Walle, and D. Vanderbilt, "Correct Implementation of Polarization Constants in Wurtzite Materials and Impact on III-Nitrides," Phys. Rev. X **6**(2), 021038 (2016).

[11] M.R. Islam, N. Wolff, M. Yassine, G. Schönweger, B. Christian, H. Kohlstedt, O. Ambacher, F. Lofink, L. Kienle, and S. Fichtner, "On the exceptional temperature stability of ferroelectric Al1-xScxN thin films," Appl. Phys. Lett. **118**(23), (2021).

[12] A. Jain, S.P. Ong, G. Hautier, W. Chen, W.D. Richards, S. Dacek, S. Cholia, D. Gunter, D. Skinner, G. Ceder, and K.A. Persson, "Commentary: The Materials Project: A materials genome approach to accelerating materials innovation," APL Mater. **1**(1), (2013).

[13] M. Noor-A-Alam, O. Z. Olszewski, and M. Nolan, "Ferroelectricity and Large Piezoelectric Response of AlN/ScN Superlattice," ACS Appl. Mater. Interfaces **11**(22), 20482–20490 (2019).

[14] S. Clima, C. Pashartis, J. Bizindavyi, S.R.C. McMitchell, M. Houssa, J. Van Houdt, and G. Pourtois, "Strain and ferroelectricity in wurtzite ScxAl1−xN materials," Appl. Phys. Lett. **119**(17), 1–5 (2021).

[15] H. Wang, N. Adamski, S. Mu, and C.G. Van de Walle, "Piezoelectric effect and polarization switching in Al1−xScxN," J. Appl. Phys. **130**(10), (2021).

[16] O. Ambacher, B. Christian, N. Feil, D.F. Urban, C. Elsässer, M. Prescher, and L. Kirste, "Wurtzite ScAlN, InAlN, and GaAlN crystals, a comparison of structural, elastic, dielectric, and piezoelectric properties," J. Appl. Phys. **130**(4), 045102 (2021).

[17] D.F. Urban, O. Ambacher, and C. Elsässer, "First-principles calculation of electroacoustic properties of wurtzite (Al,Sc)N," Phys. Rev. B **103**(11), 1–13 (2021).

[18] S. Zhang, D. Holec, W.Y. Fu, C.J. Humphreys, and M.A. Moram, "Tunable optoelectronic and ferroelectric properties in Sc-based III-nitrides," J. Appl. Phys. **114**(13), (2013).

[19] M.A. Caro, S. Zhang, T. Riekkinen, M. Ylilammi, M.A. Moram, O. Lopez-Acevedo, J. Molarius, and T. Laurila, "Piezoelectric coefficients and spontaneous polarization of ScAlN," J. Phys. Condens. Matter **27**(24), 245901 (2015).

[20] M. Akiyama, T. Kamohara, K. Kano, A. Teshigahara, Y. Takeuchi, and N. Kawahara, "Enhancement of Piezoelectric Response in Scandium Aluminum Nitride Alloy Thin Films Prepared by Dual Reactive Cosputtering," Adv. Mater. **21**(5), 593–596 (2009).

[21] L.-Q. Chen, "Phase-Field Method of Phase Transitions/Domain Structures in Ferroelectric Thin Films:

A Review," J. Am. Ceram. Soc. **91**(6), 1835–1844 (2008).

[22] K. Hirata, K. Shobu, H. Yamada, M. Uehara, S.A. Anggraini, and M. Akiyama, "Thermodynamic assessment of the Al–Sc–N ternary system and phase-separated region of the strained wurtzite phase," J. Eur. Ceram. Soc. **40**(15), 5410–5422 (2020).

[23] S. Yasuoka, R. Mizutani, R. Ota, T. Shiraishi, T. Shimizu, M. Uehara, H. Yamada, M. Akiyama, and H. Funakubo, "Tunable Ferroelectric Properties in Wurtzite (Al 0.8 Sc 0.2 )N via Crystal Anisotropy," ACS Appl. Electron. Mater. **4**(11), 5165–5170 (2022).

[24] K. Umeda, H. Kawai, A. Honda, M. Akiyama, T. Kato, and T. Fukura, in *2013 IEEE 26th Int. Conf. Micro Electro Mech. Syst.* (IEEE, 2013), pp. 733–736.

[25] P.M. Mayrhofer, H. Euchner, A. Bittner, and U. Schmid, "Circular test structure for the determination of piezoelectric constants of Sc x Al 1−x N thin films applying Laser Doppler Vibrometry and FEM simulations," Sensors Actuators A Phys. **222**, 301–308 (2015).

[26] M. Akiyama, K. Kano, and A. Teshigahara, "Influence of growth temperature and scandium concentration on piezoelectric response of scandium aluminum nitride alloy thin films," Appl. Phys. Lett. **95**(16), (2009).

[27] K.J. Choi, M. Biegalski, Y.L. Li, A. Sharan, J. Schubert, R. Uecker, P. Reiche, Y.B. Chen, X.Q. Pan, V. Gopalan, L.-Q. Chen, D.G. Schlom, and C.B. Eom, "Enhancement of Ferroelectricity in Strained BaTiO 3 Thin Films," Science (80-. ). **306**(5698), 1005–1009 (2004).

[28] J.L. Peng, Q. Li, D.L. Shan, K. Pan, G.S. Yu, and Y.Y. Liu, "Phenomenological thermodynamic potentials for bulk and thin-film Ba(Zr0.08Ti0.92)O3 single crystals," J. Appl. Phys. **119**(20), 0–5 (2016).

[29] J. Peng, D. Shan, Y. Liu, K. Pan, C. Lei, N. He, Z. Zhang, and Q. Yang, "A thermodynamic potential for barium zirconate titanate solid solutions," Npj Comput. Mater. **4**(1), (2018).

[30] Y.L. Li, L.E. Cross, and L.Q. Chen, "A phenomenological thermodynamic potential for BaTiO 3 single crystals," J. Appl. Phys. **98**(6), 0–4 (2005).

[31] M. Akiyama, K. Umeda, A. Honda, and T. Nagase, "Influence of scandium concentration on power generation figure of merit of scandium aluminum nitride thin films," Appl. Phys. Lett. **102**(2), (2013).

[32] N. Kurz, Untersuchung Der Elektro-Akustischen Und Pyroelektrischen Eigenschaften von Aluminium-Scandium-Nitrid Für Mikroakustische Hochfrequenzfilter, 2019.

[33] G. Wingqvist, F. Tasnádi, A. Zukauskaite, J. Birch, H. Arwin, and L. Hultman, "Increased electromechanical coupling in w−ScxAl1−xN," Appl. Phys. Lett. **97**(11), (2010).

[34] T. Yanagitani, and M. Suzuki, "Electromechanical coupling and gigahertz elastic properties of ScAlN films near phase boundary," Appl. Phys. Lett. **105**(12), (2014).

[35] N. Wolff, S. Fichtner, B. Haas, M.R. Islam, F. Niekiel, M. Kessel, O. Ambacher, C. Koch, B. Wagner, F. Lofink, and L. Kienle, "Atomic scale confirmation of ferroelectric polarization inversion in wurtzite-type AlScN," J. Appl. Phys. **129**(3), 034103 (2021).